Clinical Science (2019) **133** 351–365
https://doi.org/10.1042/CS20180714

PORTLAND PRESS

Research Article

SPARC is required for the maintenance of glucose homeostasis and insulin secretion in mice

Catalina Atorrasagasti[1], Agostina Onorato[1,*], María L. Gimeno[2,*], Luz Andreone[2], Mariana Garcia[1], Mariana Malvicini[1], Esteban Fiore[1], Juan Bayo[1], Marcelo J. Perone[2] and Guillermo D. Mazzolini[1]

[1]Gene Therapy Laboratory, Instituto de Investigaciones en Medicina Traslacional, Facultad de Ciencias Biomédicas, CONICET- Universidad Austral, Av. Pte. Perón 1500 (B1629AHJ) Derqui-Pilar, Buenos Aires, Argentina; [2]Instituto de Investigación en Biomedicina de Buenos Aires (IBioBA) - CONICET - Partner Institute of the Max Planck Society, Buenos Aires, Argentina

Correspondence: Guillermo D. Mazzolini (gmazzoli@austral.edu.ar)

Obesity, metabolic syndrome, and type 2 diabetes, three strongly interrelated diseases, are associated to increased morbidity and mortality worldwide. The pathogenesis of obesity-associated disorders is still under study. Secreted protein acidic and rich in cysteine (SPARC) is a matricellular glycoprotein expressed in many cell types including adipocytes, parenchymal, and non-parenchymal hepatic cells and pancreatic cells. Studies have demonstrated that SPARC inhibits adipogenesis and promotes insulin resistance; in addition, circulating SPARC levels were positively correlated with body mass index in obese individuals. Therefore, SPARC is being proposed as a key factor in the pathogenesis of obesity-associated disorders. The aim of this study is to elucidate the role of SPARC in glucose homeostasis. We show here that SPARC null (SPARC$^{-/-}$) mice displayed an abnormal insulin-regulated glucose metabolism. SPARC$^{-/-}$ mice presented an increased adipose tissue deposition and an impaired glucose homeostasis as animals aged. In addition, the absence of SPARC worsens high-fat diet-induced diabetes in mice. Interestingly, although SPARC$^{-/-}$ mice on high-fat diet were sensitive to insulin they showed an impaired insulin secretion capacity. Of note, the expression of glucose transporter 2 in islets of SPARC$^{-/-}$ mice was dramatically reduced. The present study provides the first evidence that deleted SPARC expression causes diabetes in mice. Thus, SPARC deficient mice constitute a valuable model for studies concerning obesity and its related metabolic complications, including diabetes.

Introduction

Physiological human body function is dependent on a tight control of its blood glucose levels. Glucose levels are regulated by a sophisticated network of several hormones and neuropeptides released mainly from the brain, pancreas, liver, and intestine as well as adipose and muscle tissue. In this intricate scenario, the pancreas has a key role by secreting the blood sugar-lowering polypeptide insulin and its contra-regulator glucagon. Imbalance in the relationship among hormones and peptides involved may lead to type 2 diabetes mellitus (T2DM) [1].

Obesity, which prevalence is steadily increasing in both developed and developing countries is now considered a global pandemic disease [2]; importantly, obesity is closely linked to alterations of glucose homeostasis and T2DM. Body mass index (BMI) increment above 25 kg/m^2 increases exponentially the risk of T2DM development [3]. Obesity and T2DM are linked by several factors including pro-inflammatory cytokines, insulin resistance (IR), disturbed fatty acid metabolism and cellular processes. Obesity leads to hyperinsulinemia and IR, followed by a progressive dysregulated β-cell function. Different evidences support the concept that chronic inflammation in visceral adipose tissue (but not subcutaneous adipose tissue) is the major contributor in causing IR and metabolic syndrome in the obese population [4,5].

[*] These authors contributed equally to this work.

Received: 07 August 2018
Revised: 14 December 2018
Accepted: 08 January 2019

Accepted Manuscript Online: 09 January 2019
Version of Record published: 30 January 2019

Clinical Science (2019) **133** 351–365
https://doi.org/10.1042/CS20180714

Secreted protein acidic and rich in cysteine (SPARC) is a multifunctional matricellular glycoprotein [6]. SPARC is ubiquitously expressed in different human tissues [7] and plays a key role in cellular adhesion, migration, and proliferation by regulating growth factor signaling, extracellular matrix (ECM) assembly, and cell–matrix interactions in a multi-modal manner [8]. It has been reported that SPARC expression is markedly up-regulated in the adipose tissue of obese mice [9]. In humans, circulating SPARC levels were positively correlated with BMI in obese individuals [10,11]. SPARC is secreted from adipose tissue and is predominantly derived from adipocyte, where it has a role in adipocyte differentiation, adipogenesis, and adipose tissue hyperplasia [12,13]. SPARC limits adipocyte expansion and promotes inflammation and IR [14,15], probably by altering the ECM composition needed for pre-adipocyte maturation into adipocyte. Recently, Nie *et al.* also proposed that SPARC could disrupt wnt/β-catenin signaling leading to spontaneous adipocyte differentiation [13]. Consistently, SPARC$^{-/-}$ mice exhibit increased adiposity [16] and very few studies attributed a putative role of SPARC in glucose metabolism. Pancreatic islet expressed SPARC but its role is not well characterized. SPARC is expressed by stromal cells within islets and inhibits growth factor responses and islet survival [17]. Elevated plasma levels of SPARC were detected in T2DM patients [18]. Nevertheless, Harries *et al.* reported reduced SPARC expression in primary islets from subjects with diabetes and a positive correlation between SPARC expression and glucose stimulated insulin secretion [19]. SPARC overexpression in the β cell line INS-1 increased insulin expression in high glucose conditions suggesting a direct role in insulin secretion [19]. The aim of this study was therefore to investigate the role of SPARC in the control of glucose homeostasis *in vivo*. To this end, we used SPARC knockout mice fed with normal chow diet and in a diet-induced obesity model. In this report, we show that the absence of SPARC in mice resulted in increased glycaemia and glucose intolerance in an age-dependent manner and increased predisposition to diabetes when mice received a high-fat diet. The absence of SPARC decreased insulin expression and glucose-stimulated insulin secretion, being these results more remarkable in high-fat diet-fed animals. Interestingly, glucose transporter 2 (GLUT2) expression by β cells within pancreatic islets was reduced in SPARC deficient mice. These findings highlight SPARC as a key player in glucose homeostasis.

Material and methods

Animals

SPARC knockout mice (SPARC$^{-/-}$) on a C57BL/6 background were purchased from Jackson Laboratory, U.S.A. Male SPARC$^{+/+}$ and SPARC$^{-/-}$ littermates mice were used. At 6 weeks of age SPARC$^{-/-}$ and SPARC$^{+/+}$ mice were randomized to 4 treatment groups (6–8 mice per group): group (1) SPARC$^{+/+}$ fed *al libitum* with high fat chow and 50 g/l sucrose added to drinking water (termed Western diet, WD) [16,20]; group (2) SPARC$^{+/+}$ fed *ad libitum* with regular laboratory chow (CD); group (3) SPARC$^{-/-}$ fed *al libitum* with WD; group (4) SPARC$^{-/-}$ fed *al libitum* with CD. The WD contains calcium caseinate (200 g/kg), vitamin mixture (10 g/kg), cellulose (50 g/kg), animal fat (250g/kg), vitamin A (1 ml/kg), choline bitartrate (2.5 g/kg), maltodextrin (451.5 g/kg) [16]. The mixture of vitamins and minerals are prepared according to the recommendations of the AIN 93 [21]. Animals in each group were euthanized after 12 or 20 weeks of WD or CD feeding. SPARC$^{+/+}$ and SPARC$^{-/-}$ mice fed with CD were also studies at different time point since weaning (six animals per group). All protocols dealing with animals were reviewed and approved by the Austral University Animal Studies Committee. This study followed the guidelines outlined in the National Institutes of Health Guide for the care and use of laboratory animals.

Glucose, insulin, and c-peptide measurements

Tail-vein blood samples were collected, and blood glucose levels were measured under 6-h fasting conditions with a glucose meter (OneTouch Ultra, Johnson & Johnson). For serum insulin and c-peptide, blood samples were taken in heparinized capillaries, after immediate centrifugation at 4°C, sera was separated and stored at −20°C until analysis, serum insulin and c-peptide levels were measured using a mouse insulin ELISA kit (Mercodia) or a mouse c-peptide ELISA (ALPCO). Basal insulin and c-peptide levels were measured in 6-h fasted animal. Serum insulin and c-peptide levels during intraperitoneal (i.p.) or oral tolerance test were assessed at 15 and 60 min after glucose administration.

Intraperitoneal and oral glucose tolerance tests

Animals were fasted for 6 h before i.p. glucose tolerance test (IGTT) or oral glucose tolerance test (OGTT). After a sample of fasted blood was collected, animals were given glucose (dextrose 2 g/kg body weight) by i.p. injection or by oral gavage; blood glucose readings were then taken at 15, 30 and 60 min after i.p. glucose administration or 15, 30, 60 and 120 min after oral administration.

Insulin tolerance test

For the insulin tolerance test (ITT), mice were fasted for 5 h. After a sample of fasted blood was collected, animals were injected i.p. with human insulin (1 unit/kg body weight); blood glucose readings were then taken after 30, 60, and 120 min. Blood was collected from the tail vein and blood glucose was measured using a glucose meter (OneTouch Ultra, Johnson & Johnson).

Histology and immunohistochemistry

Distal pancreas was dissected from mice, fixed in 10% phosphate-buffered formalin and dehydrated prior to paraffin embedding. Five-micrometer contiguous paraffin sections were prepared on a rotary microtome (Shandon) for H&E staining and immuno staining. Insulin was detected by immunofluorescence stain. Briefly, antigen retrieval with buffer citrate (pH = 6) was performed on tissue sections before staining. Thereafter, sections were permeabilized with 0.3% triton, blocked with 1% BSA, and incubated overnight with monoclonal mouse anti-insulin (1200; clone HB125). The antigens were visualized using appropriate secondary antibody conjugated with fluorescein FITC (1100; VECTOR). Cell nuclei were stained with DAPI (Invitrogen). Negative controls were performed in all studies. All images were digitally acquired using de same capture settings and were not further processed. Morphometric analysis for insulin-positive cells was performed using Image-J image analysis software. The intensity of insulin (mean fluorescence intensity, MFI) staining of at least five different islets in pancreatic sections from each animal were quantified by monochromatic thresholding (n=3–5 animals per group). The MFI data were corrected subtracting the background signal measured in an adjacent region of the tissue that express a noise fluorescence. To estimate the mean β-cell area, the insulin-positive area for each islet was measured, and the number of nuclei present in the insulin-stained area (μm^2) was counted to calculate the individual β-cell cross-sectional area (μm^2). For chromogenic immunohistochemical analysis and quantification of GLUT2 expression, sections were deparaffinized, rehydrated, and subject to antigen retrieval with buffer citrate (pH = 6). Endogenous peroxidase was blocked with 0.5% H_2O_2 in methanol. Tissue was then incubated with the goat anti-mouse GLUT2 polyclonal antibody (1:200; Abcam). After extensive washing, slides were incubated with peroxidase-linked biotinylated anti-goat secondary antibodies (VECTOR) for 1 h, washed and further incubated with avidin-peroxidase complex. They were then washed twice with PBS and twice with 0.1 M acetate buffer before incubation with a solution of 3.3-diaminobenzidine (DAB; Sigma), ammonium nickel sulfate and H_2O_2 until signal was developed. For controls slides, primary antibody incubation was omitted in control slides and no signal was detected. Quantitative analysis of GLUT2 immunostaining area was performed using NIH Image J software and results were expressed as positive area.

Indirect immunofluorescence for GLUT2 was performed on isolated pancreatic islets. A suspension of fresh isolated islets was permeabilized with 0.25% Triton X-100 for 10 min. Cells were sedimented at 100 G for 1 min. After blocking pellets with 1% BSA for 30 min islets were sedimented, and incubated at 4°C overnight with rabbit anti-mouse GLUT2 (1:200, Abcam). After washing, islets were incubated with anti-rabbit-FITC (Jackson ImmunoResearch). For negative controls, primary antibody was replaced with appropriate serum. The pellet was resuspended and transferred to slides. The slides were air-dried and a cover glass mounted using buffered glycerol. Images were acquired on an inverted Zeiss LSM 710 (Carl Zeiss Microscopy GmbH). Data acquisition was performed using ZEN Black 2011 software (Carl Zeiss Microscopy) and quantification using Fiji software. Mean fluorescence intensity of 15 ROI (30 × 30 μm) of each image was quantified.

Reverse transcription- real time PCR (RT-qPCR)

Total RNA was extracted from the pancreas or cell by Trizol isolation method (Life Technologies, Rockville, MD, U.S.A.). RNA (1μg) was treated with DNase (Invitrogen, U.S.A.) and RNA was reverse transcribed with 200 U of SuperScript II Reverse Transcriptase (Invitrogen, U.S.A.) using 500 ng of Oligo (dT) primers. cDNAs were subjected to qPCR and mRNA levels were quantified by SYBR® Green (Invitrogen) qPCR (Stratagene Mx3005p, Stratagene, U.S.A.) as described elsewhere. Validation of a single PCR product was performed by melting curve analysis. Relative gene expressions were calculated from the threshold cycles in relation to the reference gene glyceraldehyde-3-phosphate dehydrogenase (GAPDH) ($2^{\Delta\Delta C}{}_t$ method) using the following primers: SPARC sense (5′-CCACACGTTTCTTTGAGACC-3′); SPARC antisense (5′-GATGTCCTGCTCCTTGATGC-3′); GAPDH sense (5′-CATCTCTGCCCCCTCTGCTG -3′); GAPDH antisense (5′-GCCTGCTTCACCACCTTCTTG-3′); insulin sense (5′-GGAGCGTGGCTTCTTCTACA-3′); insulin antisense (5′-CAAGGTCTGAAGGTCCCCG-3′); Glut2 sense (5′-GGGACTTGTGCTGCTGGATA-3′); Glut2 antisense (5′-GAACACGTAAGGCCCAAGGA-3′). In all cases, the pair of primers was designed for different exons (with intronic sequences in between) to avoid amplification of genomic

Clinical Science (2019) **133** 351–365
https://doi.org/10.1042/CS20180714

DNA. Primer efficiency for all primer pair was between 98 and 112%. Results were depicted as arbitrary units related to control.

Mouse islets isolation, adenoviral infection, and glucose stimulated insulin secretion assay

Pancreatic islets were isolated from 8 to 10-week-old C57BL/6J male mice. Pancreata were inflated and digested with 2.5 mg/ml collagenase V (Sigma–Aldrich) solution, excised and incubated at 37°C in a still water bath until the exocrine tissue was approximately fully digested and purified by histopaque 1077 gradient. Islets were hand-picked under stereoscope to remove all exocrine tissue, size-matched islets (between 60 and 100 μm) were selected for each assay and O/N incubated in RPMI 1640 with GlutaMax (Gibco) supplemented with 1% P/S and 10% FBS.

Islets infection with adenovirus (MOI 50) was performed in RPMI/1% FCS during 16 h. After 72 h of infection, islets were washed in assay buffer (KRB; 135 mM NaCl, 3.6 mM KCl, 0.5 mM KH2PO4, 0.5 mM MgCl2, 10 mM HEPES, 1.5 mM CaCl2, 5 mM NaHCO3, 0.1% bovine serum albumin, pH 7.4) supplemented with 2 mM glucose. Following incubation in 2.0 mM glucose KRB for 2 h at 37°C for stabilizing the islets, islets were cultured for 1 h with 2.0 mM glucose KRB and supernantants were collected (low glucose sample). Fresh buffer was added to the cells containing either 2.0 or 20.0 mM glucose, and GSIS (glucose stimulated insulin secretion) was measured after incubation for 1 h. Cell viability of isolated pancreatic islets was ckecked by propidium iodide, and cell viability was always near 95%. The supernatant fraction was assayed for secreted insulin and the islets were collected for measurements of total protein content for normalization. Insulin concentration in supernatants was measured using a specific ELISA. The results were expressed as pg insulin/ug of total protein. Insulin secretion index was calculated as glucose (20 mM)-stimulated insulin secretion/insulin secretion at low glucose level (2 mM).

Statistical analysis

Data are expressed as mean ± S.E.M. when appropriate. Statistical significance was determined with the appropriate test depending on data distribution and number of groups. Mann–Whitney *U*-test, one-way ANOVA Kruskal–Wallis test with Dunn's multiple comparisons post-test, and factorial ANOVA were performed. For all analyses, differences were considered to be significant when $P<0.05$. For OGTT and IPGTT, the total area under the curve (AUC) for glucose concentrations was calculated individually for each animal. The results were compared group-wise. All data were analyzed using Prism version 6 software (GraphPad, Carlsbad, U.S.A.)

Results

Lack of SPARC resulted in impaired glucose homeostasis in aging mice

We and others have recently shown that SPARC$^{-/-}$ mice exhibited an age-dependent increase in visceral fat deposition; this observation led us to investigate whether glucose homeostasis might be altered in SPARC$^{-/-}$ mice [16,22]. SPARC$^{-/-}$ mice presented normal glucose levels at the time of weaning; however, significantly higher glucose levels were detected at 18-week-old compare with SPARC$^{+/+}$. To determine age-dependent changes in glucose metabolism in the absence of SPARC, fasting blood glucose was evaluated at different time points in SPARC$^{-/-}$ and SPARC$^{+/+}$ mice (6 animals per group were evaluated at different time points). Starting at a mean fasted blood glucose value of 145.4 ± 8.4 mg/dl in the 4-week-old SPARC$^{-/-}$ group, blood glucose levels increased gradually to 210 ± 5.6 mg/dl at the age of 26 weeks old (Figure 1A). As shown in Figure 1B, SPARC$^{-/-}$ mice older than 9 weeks exhibited abnormal levels of blood glucose following i.p. glucose administration, as judged by the high AUC for glucose ($AUC_{Glucose}$) in SPARC$^{-/-}$ group after 9 weeks compared with SPARC$^{+/+}$ mice (Figure 1B, upper panel). Furthermore, we carried out an IGTT in control diet (CD)-fed SPARC$^{-/-}$ mice at different ages. Eighteen- and 26-week-old SPARC$^{-/-}$ mice had normal fasting insulin content (Figure 1C, time 0) but reduced insulin increment following i.p. glucose challenge compared with SPARC$^{+/+}$ mice (Figure 1C). Fasted levels of c-peptide in 18- and 26-week-old mice were similar in both genotypes (Figure 1C). Nevertheless, c-peptide increment upon glucose stimulation was not observed at 18 and 26 weeks in SPARC$^{-/-}$ mice (Figure 1C). SPARC$^{-/-}$ mice also presented abnormally higher glucose levels after oral glucose challenge (OGTT) at week 26 compared with SPARC$^{+/+}$ mice (Figure 1D). Moreover, a significant reduction in the serum insulin and c-peptide peaks after 15 min of glucose challenge was observed in SPARC$^{-/-}$ mice at week 26 (Figure 1E). We do not observed difference in insulin expression in neonatal and 4-weeks-old SPARC$^{-/-}$ mice compared with SPARC$^{+/+}$ mice (Supplementary Figure S1). However, we observed an age-dependent decrease in pancreatic tissue insulin mRNA expression from 9-week-old onward (Figure 1F). These results demonstrated that mice lacking SPARC exhibited an age-dependent susceptibility to develop diabetes.

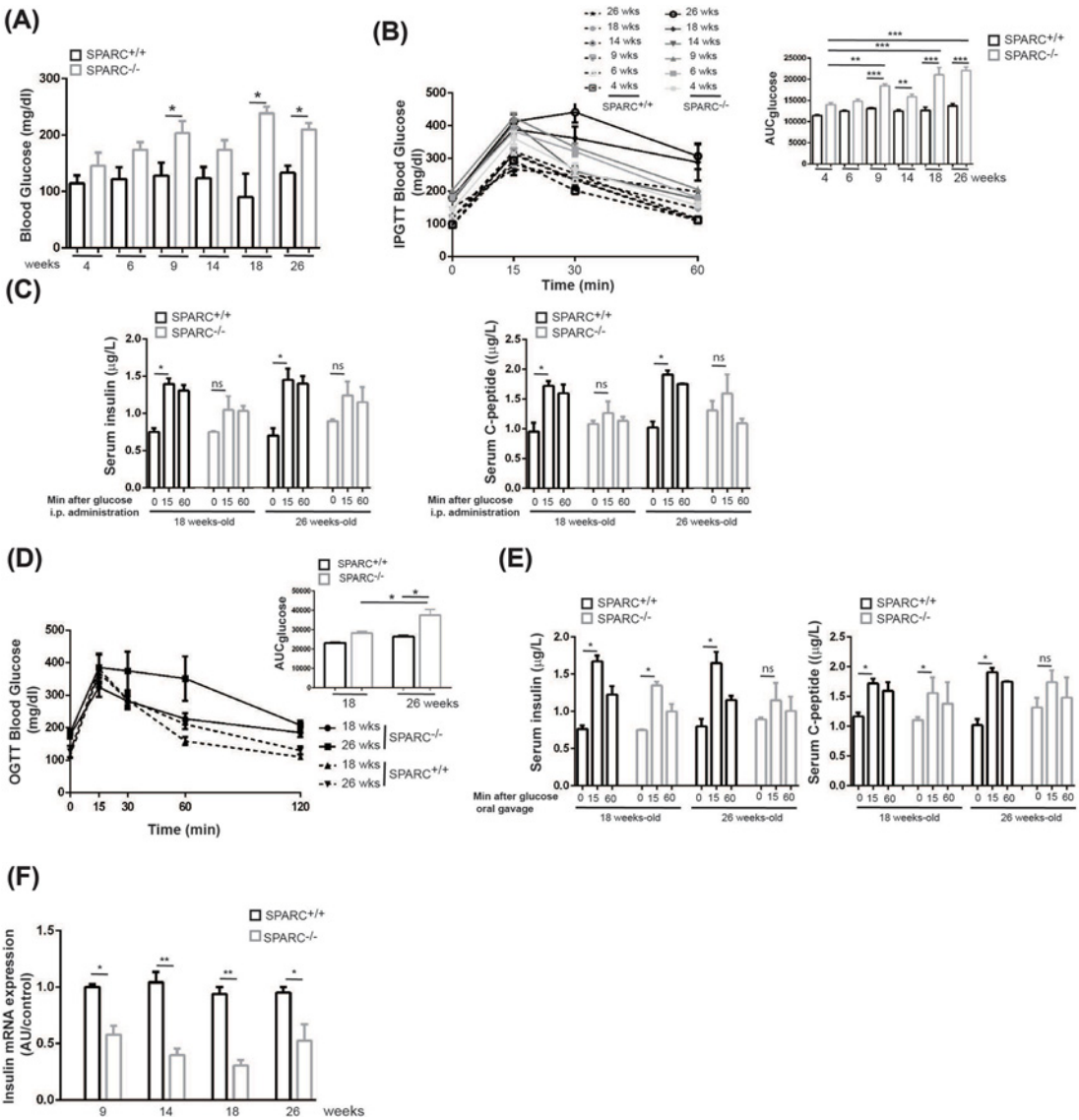

Figure 1. The absence of SPARC generates a deleterious effect on glucose homeostasis in an age-dependent manner

(**A**) Blood glucose levels in 6-h fasted SPARC$^{+/+}$ and SPARC$^{-/-}$ mice at the indicated ages. Data are shown as mean ± S.E.M. (n=6 per group). $^{*}P<0.05$, Mann–Whitney U-test. (**B**) IGTT in SPARC$^{-/-}$ (black line) and SPARC$^{+/+}$ (dotted line) mice at the indicated ages. Blood glucose levels at different time point after i.p. glucose administration. Data are shown as mean ± S.E.M. (n=6 per group). Upper panel: total AUC for glucose was calculated. Data are shown as mean ± S.E.M. (n=6 per group). $^{***}P<0.001$, $^{**}P<0.01$. Two-way ANOVA with Bonferroni's multiple comparisons test. (**C**) Serum insulin and C-peptide during IGTT. $^{*}P<0.05$, 15 min vs basal insulin or c-peptide level. Ns, non-significant difference. One-way ANOVA with Dunn's multiple comparisons test. (**D**) OGTT in 18–26-weeks-old SPARC$^{-/-}$ (black line) and SPARC$^{+/+}$ (dotted line) mice. Glycemic values before (0 min) and 15, 30, 60, 120 min after glucose oral gavage. Upper panel: total AUC for glucose was calculated. Results are means ± S.E.M. (n=6 per group). $^{*}P<0.05$. Two-way ANOVA with Bonferroni's multiple comparisons test. (**E**) Serum insulin and c-peptide during OGTT. $^{*}P<0.5$, 15 min vs basal insulin or c-peptide level. Ns, non-significant difference. One-way ANOVA Kruskal–Wallis with Dunn's multiple comparisons test. (**F**) SPARC$^{-/-}$ mice showed an age-dependent decreased in insulin mRNA expression. qPCR quantification of insulin mRNA was performed on pancreas from SPARC$^{-/-}$ at different ages. Data are shown as mean ± S.E.M. of at least three independent experiments. $^{*}P<0.05$, $^{**}P<0.01$, one-way ANOVA Kruskal–Wallis test with Dunn's multiple comparisons post-test.

Clinical Science (2019) **133** 351–365
https://doi.org/10.1042/CS20180714

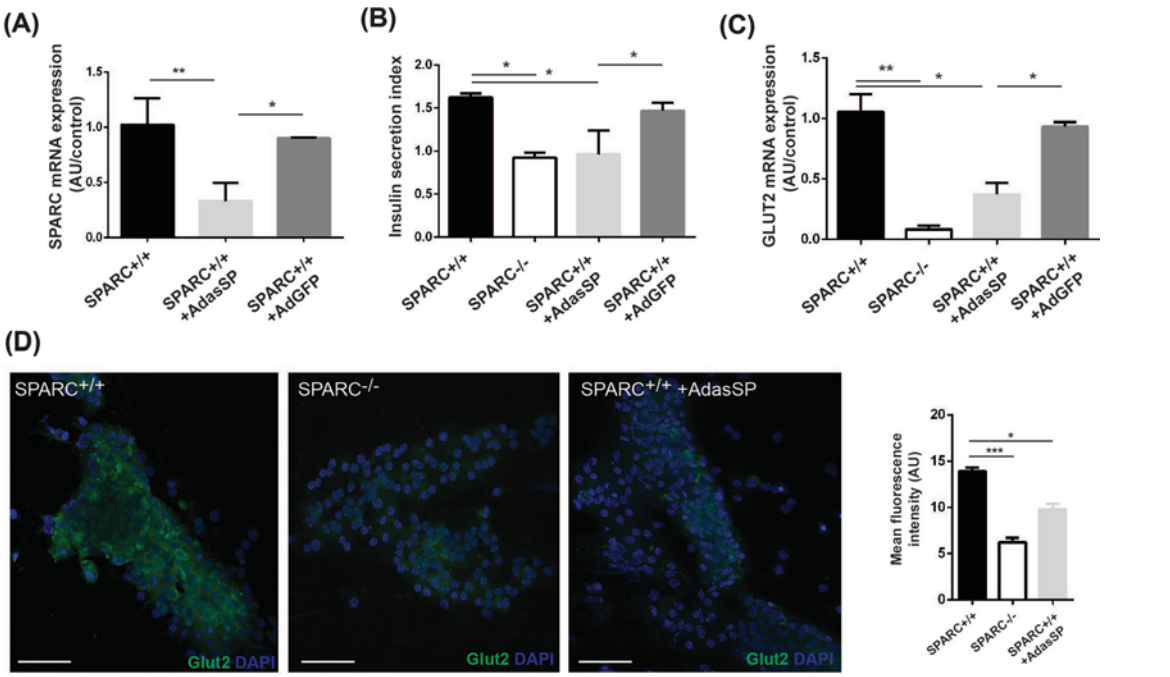

Figure 2. SPARC knockdown expression in pancreatic islets decreased glucose-stimulated insulin secretion and reduced GLUT2 expression

(**A**) qPCR quantification of SPARC mRNA before and after adenoviral infection in isolated islets. (**B**) GSIS assay in isolated mouse islets from SPARC$^{+/+}$ and SPARC$^{-/-}$ mice. Islets from SPARC$^{+/+}$ were transduced with AdasSPARC or AdGFP vector. GSIS assay was performed 72 h after. Secreted insulin was measured by ELISA in supernatants from islets cultured with low or high glucose concentration and secretion insulin index was calculated as glucose (20 mM)-stimulated insulin secretion/insulin secretion at low glucose level (2 mM). (**C**) qPCR quantification of GLUT2 mRNA expression in isolated islets before and after adenoviral infection. (**D**) Confocal microscopy of immunofluorescence staining for GLUT2 (green) and DAPI (blue) of isolated islets from SPARC$^{-/-}$, SPARC$^{+/+}$, and mice SPARC$^{+/+}$ transduced with AdasSPARC. Scale bar, 100 μm. Data are shown as mean ± S.E.M. of at least three independent experiments. $^{*}P<0.05$, $^{**}P<0.01$, one-way ANOVA Kruskal–Wallis test with Dunn's multiple comparisons post-test.

Knocking-down SPARC in islets results in diminished glucose-stimulated insulin secretion

To examine whether decrease in GSIS in SPARC-deficient mice is intrinsic to pancreatic β cells, we performed *ex vivo* GSIS analysis on isolated mouse islets. To this end, we employed a recombinant adenovirus carrying SPARC antisense mRNA (AdasSPARC) or alternatively, expressing GFP, as control (AdGFP). As shown by qPCR, isolated mouse islets expressed SPARC and AdasSPARC vector was effective to diminish SPARC expression after infection (Figure 2A). Basal insulin secretion was similar between isolated islets from SPARC$^{+/+}$ and SPARC$^{-/-}$ mice (0.16 ± 0.06 pg insulin/μg total protein and 0.12 ± 0.03 pg insulin/μg total protein respectively; Supplementary Figure S2). However, GSIS in SPARC$^{-/-}$ islets is significantly reduced in comparison with SPARC$^{+/+}$ islets (Figure 2B, Supplementary Figure S2). Likewise, genetically modified islets by SPARC antisense treatment showed impaired GSIS, confirming the role of SPARC in insulin secretion (Figure 2B).

On the other hand, it has been observed that glucagon-like peptide 1 receptor (GLP-1R) agonists potentiate glucose-stimulated insulin secretion. We assessed whether liraglutide, a GLP-1R agonist, may increase glucose-stimulated insulin secretion in SPARC$^{-/-}$ isolated islets, and observed that liraglutide failed to stimulated insulin secretion in SPARC$^{-/-}$ islets (Supplementary Figure S2).

Glucose sensing by pancreatic β cells is required for normal insulin synthesis and secretion. Glucose transport into β cells depends on GLUT2 [23]. To explore the cause of the abnormal glucose-induced insulin secretion, we investigated whether knockdown of SPARC expression could reduce GLUT2 expression in SPARC$^{+/+}$ mice. We observed that the absence of SPARC decreased GLUT2 mRNA expression (Figure 2C) and reduced GLUT2 expression in isolated SPARC$^{-/-}$ islets (Figure 2D). Similarly, AdasSPARC-infected SPARC$^{+/+}$ islets also decreased GLUT2 expression linking SPARC knockdown with GLUT2 inhibition (Figure 2C,D).

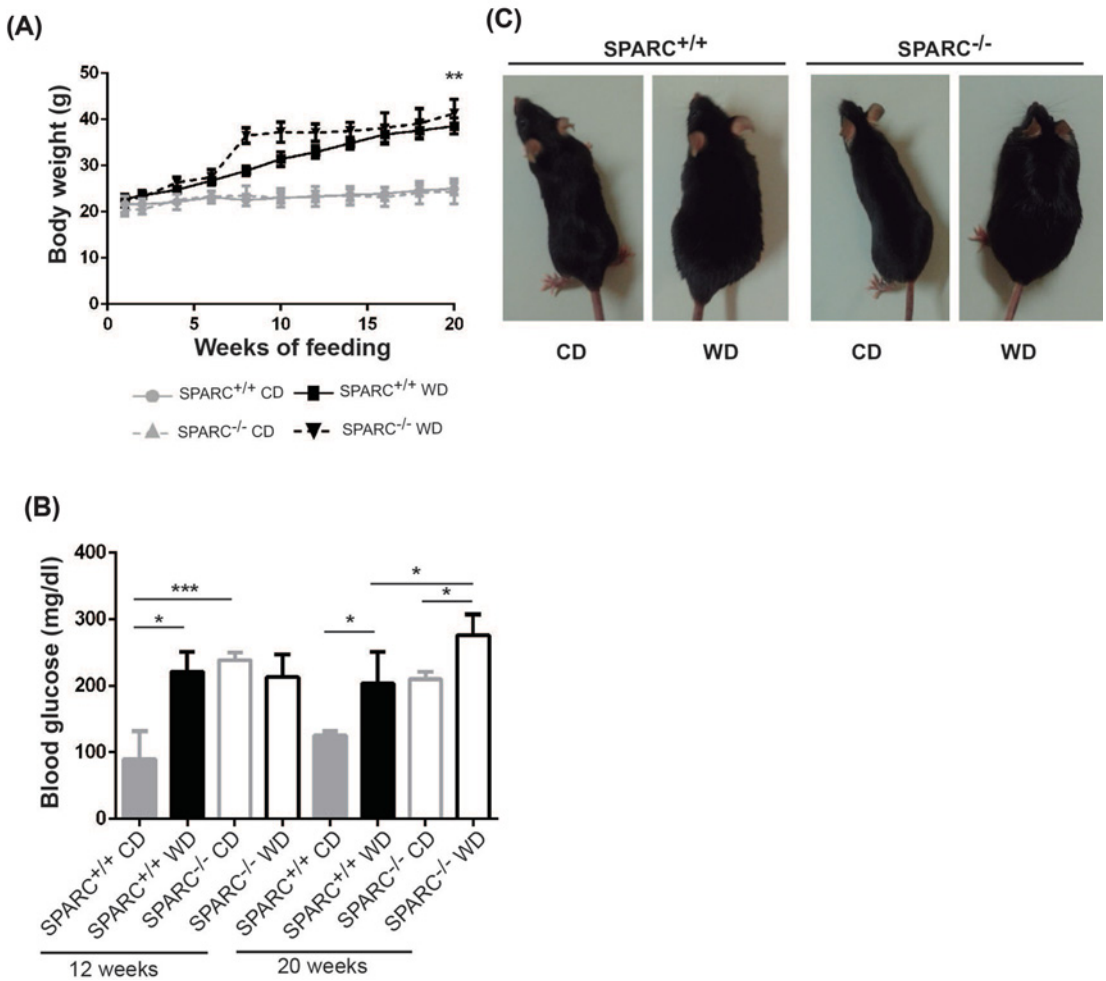

Figure 3. Body weight and blood glucose levels in SPARC$^{-/-}$ mice fed with WD

(**A**) Body weight of SPARC$^{+/+}$ and SPARC$^{-/-}$ mice fed with control diet (CD) or high fat diet plus sucrose in drinking water (WD) for 20 weeks. Six to eight mice were used to generate each time point. Error bars represent the standard error mean. $^{**}P<0.01$ compared CD vs WD groups. (**B**) Phenotypic appearance of a representative animal from each group. SPARC$^{-/-}$ mice fed with WD presented obese appearance after 20 weeks. (**C**) Fasting blood glucose levels in SPARC$^{+/+}$ and SPARC$^{-/-}$ mice after 12 or 20 weeks of CD or WD feeding. Data are expressed as mean $\pm$ S.E.M. (n=6–8 per group). $^{*}P<0.05$, $^{**}P<0.01$; two-way ANOVA with Bonferroni's multiple comparisons post-test.

Hyperglycemia and impaired glucose tolerance in SPARC$^{-/-}$ mice in response to WD-induced obesity

Obesity is one of the main causes associated with type 2 diabetes development. To test the impact of WD-induce obesity in diabetes development of SPARC$^{-/-}$ mice, we challenge these animals with a WD.

First of all, we examined weight gain in SPARC$^{+/+}$ and SPARC$^{-/-}$ mice along the time; both animal groups increased weights similarly when fed with control diet (CD). In addition, both SPARC$^{+/+}$ and SPARC$^{-/-}$ mice significantly increased weight when fed with a WD compared with CD (Figure 3A,B). No significantly differences between WD-fed SPARC$^{+/+}$ and SPARC$^{-/-}$ mice body weight were observed, although, as we reported previously, SPARC$^{-/-}$ mice showed clearly more visceral fat deposition even when feeding with a CD [16]. We first measured blood glucose concentration in SPARC$^{+/+}$ and SPARC$^{-/-}$ mice after feeding 6-week-old animals with CD or WD for 12 or 20 weeks. In accordance with our previously results, glucose levels were increased in CD-fed SPARC$^{-/-}$ mice compared with CD-fed SPARC$^{+/+}$. As expected, WD-fed SPARC$^{+/+}$ mice increased glucose levels compared with CD-fed SPARC$^{+/+}$ mice, but this increase was significantly higher in WD-fed SPARC$^{-/-}$ mice after 20 weeks (Figure 3C). In line with this, SPARC$^{-/-}$ mice challenged i.p. with glucose showed remarkable glucose intolerance ($AUC_{glucose}$

Clinical Science (2019) **133** 351–365
https://doi.org/10.1042/CS20180714

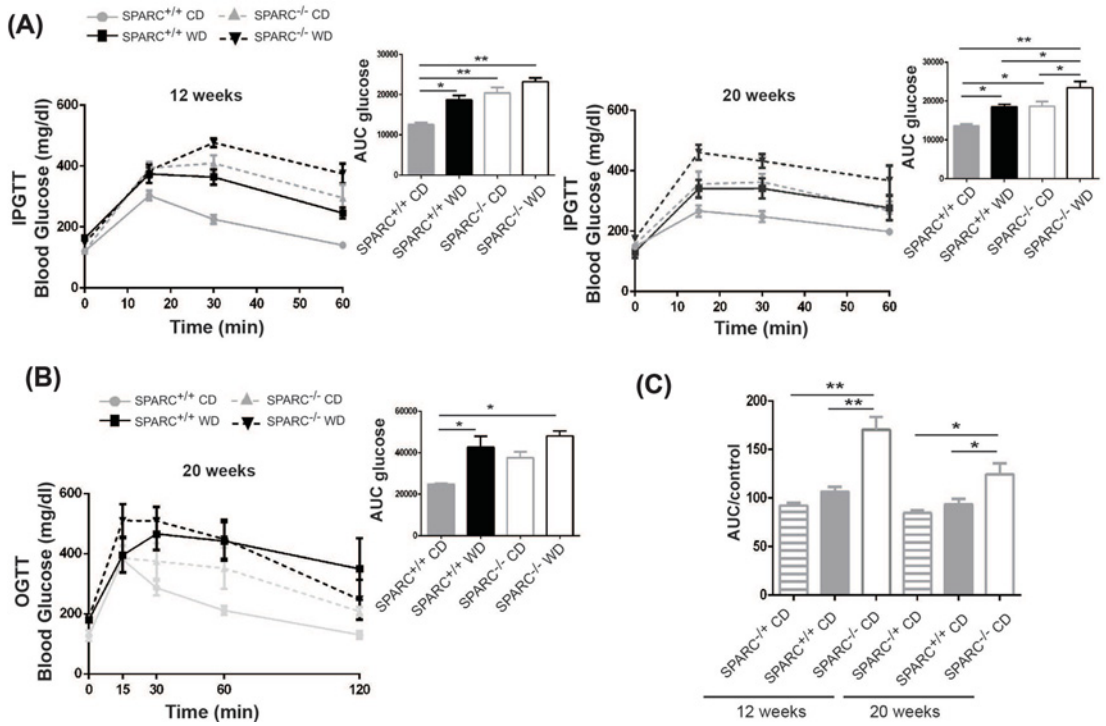

Figure 4. WD-fed SPARC$^{-/-}$ mice showed glucose intolerance

(**A**) IGTT were conducted in SPARC$^{+/+}$ and SPARC$^{-/-}$ mice, feed with CD or WD for 12 or 20 weeks, after a period of 6h fasting. Kinetics of blood glucose changes during IGTT (left panels) and AUC quantification of the glucose tolerance tests of each group (upper panels). Data are expressed as mean ± S.E.M. (n=6–8 per group). $^{*}P<0.05$, $^{**}P<0.01$; two-way ANOVA test with Bonferroni's multiple comparisons post-test. (**B**) Plasma glucose during the OGTT in SPARC$^{+/+}$ and SPARC$^{-/-}$ mice, feed with CD or WD for 20 weeks. AUC for glucose was calculated (upper panel). Data are expressed as mean ± S.E.M. (n=4–6 per group) $^{*}P<0.05$; two-way ANOVA test with Bonferroni's multiple comparisons post-test. (**C**) Heterozygote CD-fed mice (SPARC$^{+/-}$) showed a preserved tolerance to glucose. AUC of IGTT of SPARC$^{+/-}$ mice. Data are expressed as mean ± S.E.M. (n=6–8 per group). $^{*}P<0.05$, $^{**}P<0.01$; one-way ANOVA Kruskal–Wallis test with Dunn's multiple comparisons post-test.

= 20463 ± 1353 SPARC$^{-/-}$CD vs. $AUC_{glucose}$ = 12623 ± 480 SPARC$^{+/+}$CD, $P<0.01$, 12 weeks; $AUC_{glucose}$ = 18670 ± 1216 SPARC$^{-/-}$CD vs. $AUC_{glucose}$ = 13674 ± 418 SPARC$^{+/+}$CD, $P<0.05$, 20 weeks), being this effect greater in WD-fed SPARC$^{-/-}$ mice both at 12 and 20 weeks ($AUC_{glucose}$ = 23235 ± 927 SPARC$^{-/-}$WD vs. $AUC_{glucose}$ = 12623 ± 479 SPARC$^{+/+}$CD, $P<0.01$, 12 weeks; $AUC_{glucose}$ = 23467 ± 1592 SPARC$^{-/-}$WD vs. $AUC_{glucose}$ = 13674 ± 416 SPARC$^{+/+}$CD, $P<0.01$, 20 weeks) (Figure 4A). When OGTT assay was performed at 20 week after CD or WD feeding, similar results were obtained but no significant difference between SPARC$^{+/+}$CD and SPARC$^{-/-}$CD was observed ($AUC_{glucose}$ = 37637 ± 2839 SPARC$^{-/-}$CD vs. $AUC_{glucose}$ = 24814 ± 508 SPARC$^{+/+}$CD, $P<0.05$; $AUC_{glucose}$ = 48080 ± 2458 SPARC$^{-/-}$WD vs. $AUC_{glucose}$ = 24814 ± 508 SPARC$^{+/+}$CD, $P<0.05$) (Figure 4B). Of note, heterozygote CD-fed mice (SPARC$^{+/-}$) presented similar glucose levels after i.p. glucose administration in comparison with SPARC$^{+/+}$ mice (Figure 4C).

Normal pancreatic histology but decreased insulin expression in SPARC$^{-/-}$ mice

To explain the high levels of glycaemia and glucose intolerance, we decided to analyze β cells in pancreatic islets in SPARC$^{-/-}$ mice. Histological analysis did not reveal any significant difference in islet shape or size, nor with the presence of inflammatory cells (Figure 5A). To assess changes in normal distribution of α and β cells between SPARC$^{-/-}$ and control mice, we performed immunofluorescence staining for insulin and glucagon. As a result, we did not observe any significant difference in glucagon and insulin positive cells ratio between pancreas of SPARC$^{+/+}$ and SPARC$^{-/-}$ mice fed with CD (Supplementary Figure S3). To test the capacity of the islets to produce insulin, we first examined insulin expression by qPCR and observed that insulin mRNA level was decreased in the pancreas of 20

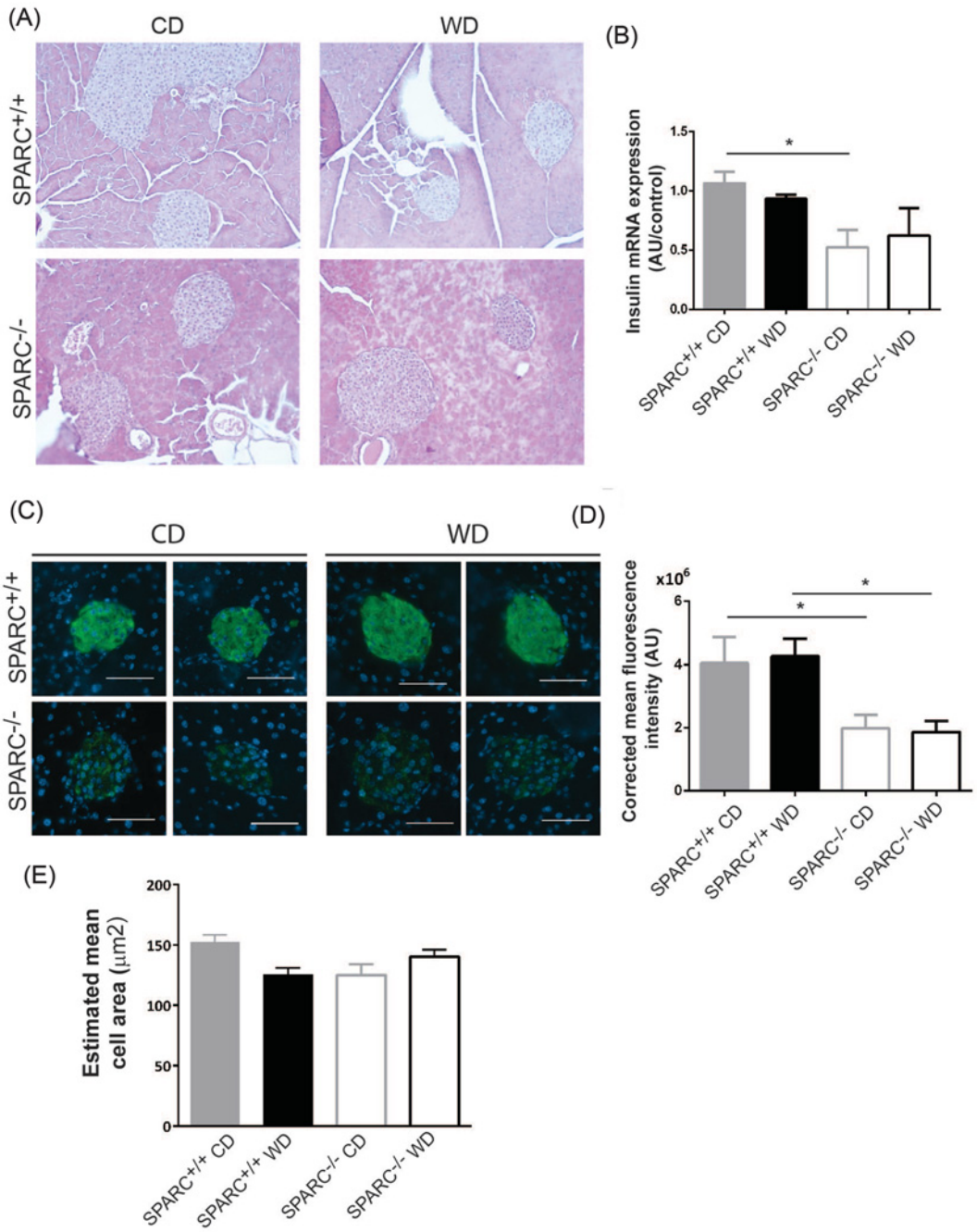

Figure 5. Islets morphology and insulin expression in SPARC$^{-/-}$ mice

(**A**) Islets were morphologically well preserved in SPARC$^{-/-}$ mice. Representative haematoxylin-eosin staining images of pancreas sections from SPARC$^{+/+}$ and SPARC$^{-/-}$ mice fed with CD or WD for 20 weeks. Amplification, 100×. (**B**) Insulin mRNA expression was down-regulated in SPARC$^{-/-}$ mice. qPCR for insulin from pancreas samples from SPARC$^{+/+}$ and SPARC$^{-/-}$ mice fed with CD or WD for 20 weeks. (**C**) Insulin staining was decreased in islets from SPARC$^{-/-}$ mice. Representative immunofluorescence images of pancreas sections from SPARC$^{+/+}$ and SPARC$^{-/-}$ mice fed with CD or WD for 20 weeks. Islets were stained with anti-insulin antibody (green) and DAPI (blue). Scale bar, 50 µm. (**D**) Quantification of fluorescence intensity of insulin. 5–10 islets per animal were analyzed (n=3–5 animals per group). Data are expressed as mean ± S.E.M. $^{*}P<0.05$, two-way ANOVA test with Bonferroni's multiple comparisons post-test. (**E**) The mean β cell area was similar between both SPARC$^{-/-}$ and SPARC$^{+/+}$ mice. Morphometric analysis of insulin positive area of five islets per mouse (n=3–5). Data are expressed as mean ± S.E.M.

Clinical Science (2019) **133** 351–365
https://doi.org/10.1042/CS20180714

weeks CD-fed SPARC$^{-/-}$ mice; no significant differences were observed between SPARC$^{-/-}$ and SPARC$^{+/+}$ mice fed with WD (Figure 5B). At the protein level, immunoreactive-insulin was decreased significantly (∼2-fold) within islets of SPARC$^{-/-}$ in comparison with SPARC$^{+/+}$ mice, independently of the assigned diet (Figure 5C,D). Heterozygote mice (SPARC$^{+/-}$) presented similar insulin staining in comparison with SPARC$^{+/+}$ mice (data not shown). When we studied the mean β cell area no significantly differences were observed, indicating no changes in β cell mass (Figure 5E).

SPARC deficiency causes insulin secretory impairment in response to glucose stimulation

The above results suggest that the absence of SPARC is involved in the decreased insulin expression in β cells. Nevertheless, fasting insulin and c-peptide serum levels did not differ between SPARC$^{+/+}$ and SPARC$^{-/-}$ CD-fed mice (Figure 6A, upper panel). Interestingly, when SPARC$^{-/-}$ mice were fed with WD for 20 weeks did not increase fasting insulin serum levels or c-peptide; while, as expected, WD-fed SPARC$^{+/+}$ mice developed hyperinsulinemia (Figure 6A, upper panel). To determine whether the absence of SPARC alters glucose-stimulated insulin secretion, we measured insulin and c-peptide serum levels in response to i.p. and oral glucose challenge. Remarkable, we obtained similar results independent of the route of administration. As expected, CD-fed SPARC$^{+/+}$ mice responded to glucose challenge increasing serum insulin and c-peptide levels, while WD-fed SPARC$^{+/+}$ mice did not response properly to glucose stimulation (Figure 6A,B). Of note, SPARC$^{-/-}$ mice did not secrete insulin and c-peptide in response to a glucose demand, independently of the diet assigned, and respond in this sense similarly as wild-type mice fed with WD (Figure 6A,B). Insulin secretion index was calculated as insulin concentration 15 min after glucose i.p. administration/basal fasting insulin levels. Insulin secretion index was enhanced in CD-fed SPARC$^{+/+}$ mice compared with WD-fed SPARC$^{+/+}$ mice (2.83 $\pm$ 0.9 vs 0.91 $\pm$ 0,3, respectively), whereas no significant changes were observed between CD and WD-fed SPARC$^{-/-}$ mice (1.6 $\pm$ 0.7 vs 0.87 $\pm$ 0.2, respectively) (Figure 6C).

To investigate the ability of insulin to metabolize glucose in SPARC$^{-/-}$ mice, we performed an ITT. As it was expected WD-fed SPARC$^{+/+}$ mice displayed an impaired insulin-stimulated glucose blood clearance at 20 weeks; however, CD and WD-diet fed SPARC$^{-/-}$ mice remained sensitive to insulin as indicated by glucose drop levels in the ITT assay (Figure 6D).

Altered β islets GLUT2 expresssion in SPARC$^{-/-}$ mice

Next, we analyzed GLUT2 expression in pancreatic tissue by qPCR and immunohistochemistry. GLUT2 mRNA expression was not altered among groups; however, as we previously observed in isolated islets, SPARC$^{-/-}$ mice exhibited a dramatic decreased in GLUT2 immunoreactivity in comparison with SPARC$^{+/+}$ mice, independently of diet assigned (Figure 7A,B). The same decrease in GLUT2 expression was observed in pancreas of SPARC$^{-/-}$ mice compared with pancreas of SPARC$^{+/+}$ mice by WD (Figure 7C,D).

Discussion

We herein show that SPARC$^{-/-}$ mice showed increased blood glucose levels and impaired glucose tolerance in an age-dependent manner. In addition, SPARC$^{-/-}$ mice exhibit increased adipose tissue deposit during their normal development. To further investigate these metabolic alterations, we challenged SPARC$^{-/-}$ mice to a WD-induced obesity model. Being obese increases the risks of developing type 2 diabetes, and to gain further insight into the physiological role of SPARC in the glucose homeostasis we assessed glycaemia, glucose tolerance and insulin-stimulated glucose clearance in SPARC$^{-/-}$ and WD-fed SPARC$^{-/-}$ mice. We and others have recently shown that the absence of SPARC resulted in accelerated adipose tissue deposition in a diet-induced obesity model [14,16]. When fed with a WD, SPARC$^{-/-}$ mice ingested similar amounts of calories as SPARC$^{+/+}$ mice but showed significantly more visceral fat accumulation [22]. Moreover, the metabolic alterations observed in SPARC$^{-/-}$ mice were aggravated following WD feeding. In this work, we demonstrated that SPARC is required for proper insulin secretion in response to glucose stimulation, although SPARC$^{-/-}$ mice remained responsive to insulin and no clear evidence of IR was observed. Importantly, our data suggest that SPARC regulates β cell glucose sensing, at least in part, through maintaining normal GLUT2 expression levels in β cells.

SPARC has been reported to be up-regulated in adipose tissue of obese mice [9,15] and in serum of obese patients [10,11]. It has been observed that SPARC limits adipose-tissue expansion but promotes inflammation and IR [15,24]. SPARC overexpression in 3T3-L1 adipocyte cell line reduces insulin-stimulated glucose uptake by a reduction in GLUT4 transporter expression [15]. In L6 myocytes, SPARC also affects AMPK-mediated glucose metabolism

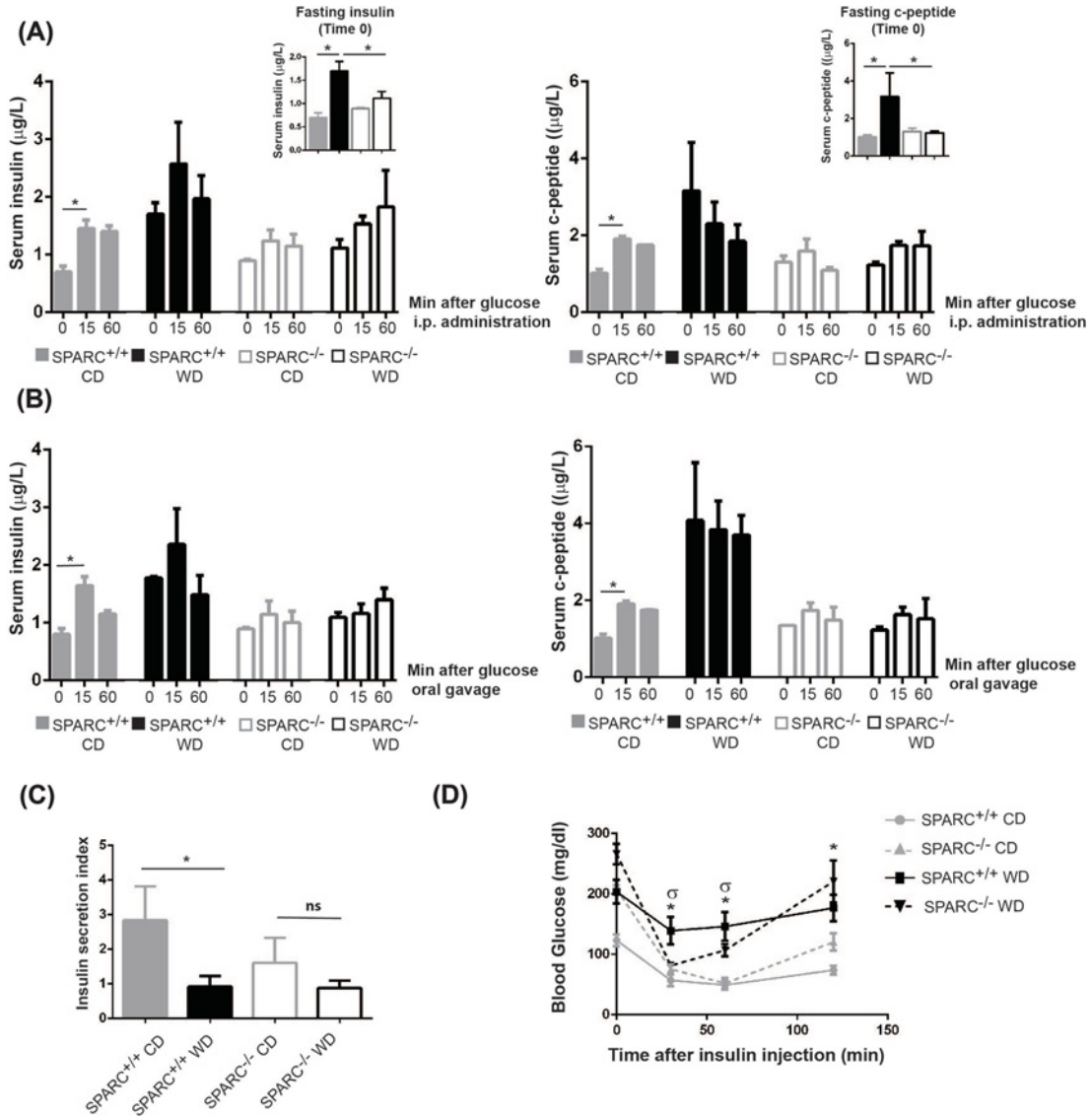

Figure 6. Glucose-stimulated insulin secretion is impaired in SPARC$^{-/-}$ mice challenged with WD

Serum insulin and c-peptide concentrations during IGTT (**A**) or OGTT (**B**) in SPARC$^{+/+}$ and SPARC$^{-/-}$ mice fed with control diet (CD) or western diet (WD) for 20 weeks. Insulin and c-peptide levels were measured prior to glucose administration and after 15 and 60 min. Data are expressed as mean ± S.E.M. (n=4 animals per group). $^{*}P<0.05$, 15 min vs basal levels, one-way ANOVA Kruskal–Wallis test with Dunn's multiple comparisons post-test. Upper panel: fasting insulin and c-peptide concentrations prior glucose administration. $^{*}P<0.05$; one-way ANOVA Kruskal–Wallis test with Dunn's multiple comparisons post-test. (**C**) Insulin secretion index was calculated as serum insulin level after 15 min of intraperitoneal administration of 2 g/kg dextrose/basal 6-h fasting insulin level. Data are shown as mean ± S.E.M. (n=6 animals per group). $^{*}P<0.05$, two-way ANOVA test with Bonferroni's multiple comparisons post-test. ns, non-significant difference. (**D**) Intraperitoneal ITT were performed in SPARC$^{+/+}$ and SPARC$^{-/-}$ mice after 20 weeks of CD or WD feeding. $^{*}P<0.05$, compared CD-fed SPARC$^{+/+}$ vs WD-fed SPARC$^{+/+}$, $^{\sigma}P<0.05$, compared WD-fed SPARC$^{+/+}$ vs WD-fed SPARC$^{-/-}$. Data are expressed as mean ± S.E.M. (n=6–8 per group). Two-way ANOVA test with Bonferroni's multiple comparisons post-test.

through regulation of GLUT4 expression [25]. In our study, we found that SPARC$^{-/-}$ mice showed increased glycaemia but do not present alteration in insulin-stimulated glucose clearance, even when SPARC deficiency increased visceral fat including the liver [16]. Although we do not assessed insulin sensitivity in skeletal muscle and adipose tissue the ITT assay demonstrated that SPARC$^{-/-}$ mice remained insulin sensitive.

Clinical Science (2019) **133** 351–365
https://doi.org/10.1042/CS20180714

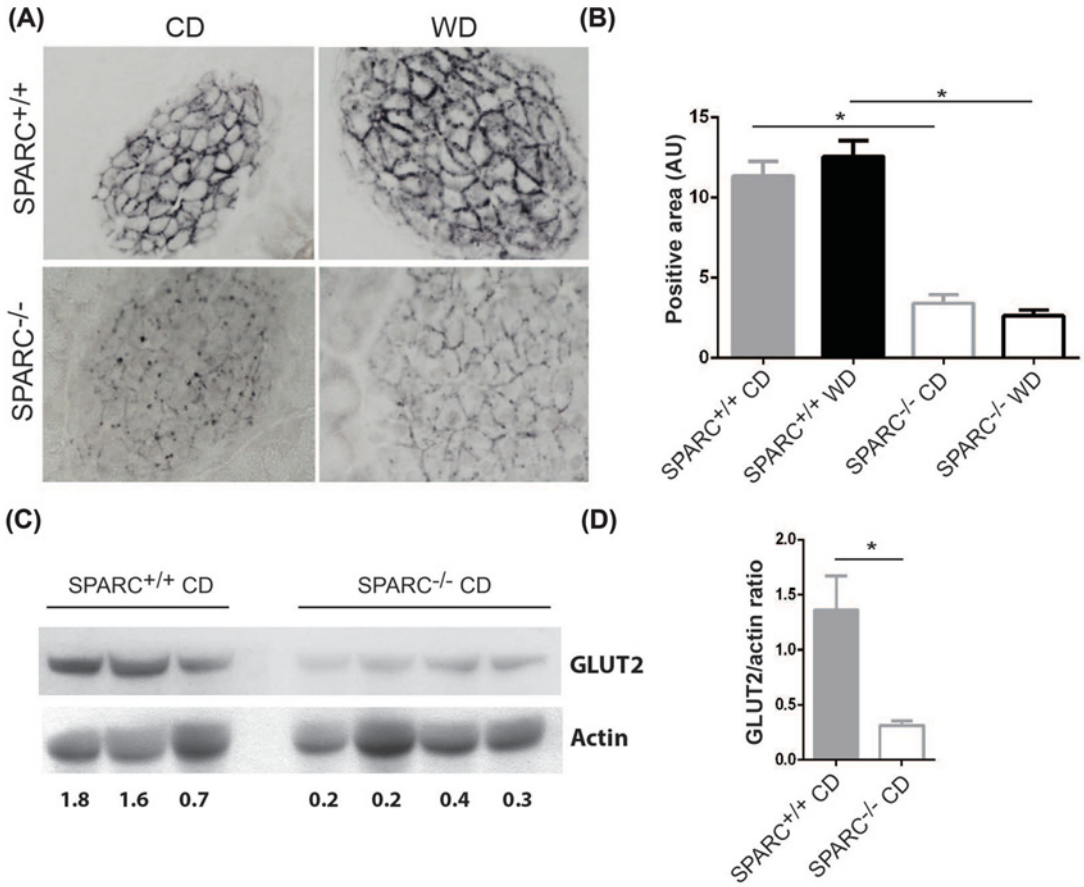

Figure 7. Low GLUT2 expression levels in SPARC$^{-/-}$ mice challenged with WD

(**A**) Immunodetection of GLUT2 in pancreatic sections of SPARC$^{+/+}$ and SPARC$^{-/-}$ CD or WD-fed for 20 weeks. Amplification, 200×. (**B**) Quantification of the GLUT2 stained area. Data are shown as mean ± S.E.M. $^{*}P<0.05$, one-way ANOVA Kruskal–Wallis test with Dunn's multiple comparisons post-test. (**C**) Western blot analyses for GLUT2 of pancreatic tissue from SPARC$^{+/+}$ and SPARC$^{-/-}$ mice (CD-fed). The same blot was subsequently hybridized with an anti-actin antibody to verify loading. (**D**) Quantification of the GLUT2/actin ratio. Data are shown as mean ± S.E.M. $^{**}P<0.01$, Mann–Whitney test.

SPARC is expressed in human islets [19], mainly by stromal cells, but its role in β cell physiology is not clearly understood yet. SPARC has been recently identified as a regulator of β cell growth and survival by inhibiting growth factor-induced signaling and IGF-induced proliferation [17]. SPARC expression positively correlated with glucose-stimulated insulin secretion in human primary pancreatic islets cultures [19]. Furthermore, overexpression of SPARC in cultured rat β cells (INS-1 cell line) increased glucose-stimulated insulin secretion [19]. In our study, the absence of SPARC did not alter the normal morphology or the total number of β cells within islets of CD- or WD-fed mice. Indeed, α/β cell ratio was similar in SPARC$^{+/+}$ and SPARC$^{-/-}$ CD-fed mice. Interestingly, SPARC$^{-/-}$ mice presented a decreased insulin expression as revealed by immunofluorescence, although basal serum insulin level was normal even in mice fed with WD. Nonetheless, CD and WD-fed SPARC$^{-/-}$ mice showed a clear impaired glucose tolerance test. To address this issue, we studied serum insulin and c-peptide levels in response to glucose stimulus and found that SPARC$^{-/-}$ mice loss the capacity of glucose-stimulated insulin secretion as happen with diabetic mice. SPARC could be playing a role in regulating β cell function by several potential mechanisms. Interestingly, SPARC down-regulation in isolated β islets also decreased glucose-stimulated insulin secretion suggesting that the role of SPARC on insulin secretion is not critical during development. Harries *et al*. observed that insulin secretion is increased in SPARC-transfected rat β cells in response to IBMX/Forskolin suggesting that the mode of action may involve alternative regulatory pathways that might act by increasing the effect of high cellular calcium concentration on insulin vesicle exocytosis once glucose has reached a threshold value [26]. On the other hand, it is known that interactions between islet cells and ECM may regulate multiple aspects of islet physiology, including

GLUT2 expression that is required for normal glucose sensing in β cells [27]. In line with this, we observed that the absence of SPARC decreased GLUT2 expression in β cells, indicating an important deficiency in the glucose sensing machinery. SPARC$^{-/-}$ mice share some common characteristics with GLUT2$^{-/-}$ mice, such as hyperglycemia and impaired glucose tolerance. However, GLUT2$^{-/-}$ mice were unable to survive after the third week of life. GLUT2$^{-/-}$ mice are hypoinsulinemic, and their β cells have lost the first phase of insulin secretion in response to glucose stimuli. Moreover, islets of Langerhans of GLUT2$^{-/-}$ mice showed an inversion of the α/β cell ratio with an absolute increase in α cell number, and a decreased in β cell number [28,29]. This feature is not altered in SPARC$^{-/-}$ mice which do not present alteration α/β cell ratio, present normal viability, and do not present hypoinsulinemia in the fasted state. Regarding other GLUT, as we discussed previously, in myocytes SPARC is involved in AMPKα phosphorylation and increases GLUT4 expression [25]. These findings support SPARC as a player in GLUT4 regulation. It would be interesting to investigate whether the absence of SPARC affects the expression of other GLUTs in peripheral tissues. Further studies on other GLUT are needed to assess whether SPARC has a role in glucose sensing.

Liraglutide increased glucose-stimulated insulin secretion in SPARC$^{+/+}$ isolated islets, but not in SPARC$^{-/-}$-derived islets. It is known that GLP1-induced insulin release is dependent upon glucose-initiated events, and cannot be mediated without a glucose stimulus [30]. Insulin secretion induced by GLP-1R agonists has been shown to be dependent, *in vitro* and *in vivo*, on β-cell detection of elevated glucose concentrations. Thus, our result provides more evidences regarding the deficiencies in insulin secretion and glucose sensing observed in SPARC$^{-/-}$ mice.

SPARC could also be affecting β-cell function by modulating the differentiation state of pancreatic β cells. It is known that β-cell development during embryogenesis and IR-induced neogenesis of β cells may be affected by the activity of several metalloproteinases [31,32]. Several metalloproteinases, involved in remodeling and degradation of ECM components, are regulated by SPARC [33]. Moreover, Ryall *et al.* recently proposed stromal-derived SPARC protein as novel regulator of islets growth and survival during development [17]. In our study, we did not observe changes in glycaemia, morphology, or insulin synthesis in SPARC$^{-/-}$ newborn mice, suggesting that there are no substantial alterations in β cell development during embryogenesis. However, SPARC$^{-/-}$ mice older than 18 weeks exhibited abnormal IGTT. A decreased insulin mRNA expression was also observed from 9-week-old mice. These results demonstrated that the absence of SPARC increases diabetic susceptibility in an age-dependent manner.

It is also known that integrin–ECM interactions are regulators of the β cell function [34]. In particular, it has been reported that β1-integrin promotes insulin expression and secretion [35,36]. In ovarian cancer, SPARC has been identified as a negative regulator of integrin β1-mediated adhesion [37]. Taken this data together, the role of SPARC in β1-integrin signaling in β cell merits further investigation.

In summary, this work describes a key role for SPARC in insulin secretion and glucose homeostasis in mice. All in all, our data demonstrated that SPARC is necessary to regulate insulin expression and secretion. The absence of SPARC in mice resulted in increased glycaemia and glucose intolerance in an age-dependent manner and led to diabetes development when mice received a WD. The effects of SPARC inhibition on the presence of GLUT2 in pancreatic islets deserve a study in depth. Therefore, it is important to further investigate the intimate mechanisms by which SPARC regulates β cell function.

Clinical perspectives

- SPARC is being proposed as a key factor in the pathogenesis of obesity-associated disorders. SPARC inhibits adipogenesis and promotes IR. Mice deficient for SPARC develop obesity. However, the role of SPARC in the control of glucose homeostasis is unknown.
- The absence of SPARC in mice resulted in increased glycemia and glucose intolerance in an age-dependent manner. The absence of SPARC worsens high-fat diet-induced diabetes in mice. SPARC inhibition reduced GLUT2 expression in β cell and impaired insulin secretion capacity.
- Strategies aimed at investigating the role of SPARC in clinical situations in which insulin secretion is impaired merits further investigation.

Clinical Science (2019) **133** 351–365
https://doi.org/10.1042/CS20180714

Acknowledgements

We thank A. Suburo and T. Bachor (Instituto de Investigaciones en Medicina Traslacional, Facultad de Ciencias Biomédicas, CONICET- Universidad Austral) for kindly providing GLUT2 antibody. We thank Guillermo Gaston for technical assistance. We would also like to thank D.Cragnolini, Dr M. Contardi and M. Namia for expert technical assistance in ^{18}F-FDG biodistribution assay.

Funding

The present study was supported by grants from Austral University [grant numbers: T-80020160300013UA-16 (to C.A.) and I-80020170100010UA-17 (to A.O.)] and from Agencia Nacional de Promociones Científicas y Tecnológicas (ANPCyT) grants [grant numbers: PICT2014-2666 (to C.A.); PICT2015-2036 (to G.M.); and PICTO2016-0101].

Competing interests

The authors declare that there are no competing interests associated with the manuscript.

Author contribution

C.A., A.O., M.G., L.A., M.G., M.M., E.F., and J.B. contributed to the acquisition and analysis of data. C.A. and G.M. contributed to the critical interpretation of the results. C.A., G.M., and M.P. participated in the drafting and writing of the manuscript. All authors critically revised the manuscript and approved the final version. G.M. is the guarantor of this work.

Abbreviations

AMPK, AMP-activated protein kinase; BMI, body mass index; CD, control diet; ECM, extracellular matrix; GAPDH, glyceraldehyde-3-phosphate dehydrogenase; GLP-1R, glucagon-like peptide 1 receptor; GLUT2, glucose transporter 2; GSIS, glucose stimulated insulin secretion; IGF, insulin-like growth factor; IGTT, i.p. glucose tolerance test; i.p., intraperitoneal; IR, insulin resistance; ITT, insulin tolerance test; MFI, mean fluorescence intensity; OGTT, oral glucose tolerance test; T2DM, type 2 diabetes mellitus; SPARC, secreted protein acidic and rich in cysteine; WD, western diet.

References

1 Roder, P.V., Wu, B., Liu, Y. and Han, W. (2016) Pancreatic regulation of glucose homeostasis. *Exp. Mol. Med.* **48**, e219, https://doi.org/10.1038/emm.2016.6
2 Ng, M., Fleming, T., Robinson, M., Thomson, B., Graetz, N., Margono, C. et al. (2014) Global, regional, and national prevalence of overweight and obesity in children and adults during 1980-2013: a systematic analysis for the Global Burden of Disease Study 2013. *Lancet* **384**, 766–781, https://doi.org/10.1016/S0140-6736(14)60460-8
3 Bano, G. (2013) Glucose homeostasis, obesity and diabetes. *Best Pract. Res. Clin. Obstet. Gynaecol.* **27**, 715–726, https://doi.org/10.1016/j.bpobgyn.2013.02.007
4 Reaven, G.M. (1995) Pathophysiology of insulin resistance in human disease. *Physiol. Rev.* **75**, 473–486, https://doi.org/10.1152/physrev.1995.75.3.473
5 Preis, S.R., Massaro, J.M., Robins, S.J., Hoffmann, U., Vasan, R.S., Irlbeck, T. et al. (2010) Abdominal subcutaneous and visceral adipose tissue and insulin resistance in the Framingham heart study. *Obesity* **18**, 2191–2198, https://doi.org/10.1038/oby.2010.59
6 Termine, J.D., Kleinman, H.K., Whitson, S.W., Conn, K.M., McGarvey, M.L. and Martin, G.R. (1981) Osteonectin, a bone-specific protein linking mineral to collagen. *Cell* **26**, 99–105, https://doi.org/10.1016/0092-8674(81)90037-4
7 Rivera, L.B., Bradshaw, A.D. and Brekken, R.A. (2011) The regulatory function of SPARC in vascular biology. *Cell. Mol. Life Sci.* **68**, 3165–3173, https://doi.org/10.1007/s00018-011-0781-8
8 Bradshaw, A.D. (2012) Diverse biological functions of the SPARC family of proteins. *Int. J. Biochemi. Cell Biol.* **44**, 480–488, https://doi.org/10.1016/j.biocel.2011.12.021
9 Tartare-Deckert, S., Chavey, C., Monthouel, M.N., Gautier, N. and Van Obberghen, E. (2001) The matricellular protein SPARC/osteonectin as a newly identified factor up-regulated in obesity. *J. Biol. Chem.* **276**, 22231–22237, https://doi.org/10.1074/jbc.M010634200
10 Kos, K., Wong, S., Tan, B., Gummesson, A., Jernas, M., Franck, N. et al. (2009) Regulation of the fibrosis and angiogenesis promoter SPARC/osteonectin in human adipose tissue by weight change, leptin, insulin, and glucose. *Diabetes* **58**, 1780–1788, https://doi.org/10.2337/db09-0211
11 Takahashi, M., Nagaretani, H., Funahashi, T., Nishizawa, H., Maeda, N., Kishida, K. et al. (2001) The expression of SPARC in adipose tissue and its increased plasma concentration in patients with coronary artery disease. *Obes. Res.* **9**, 388–393, https://doi.org/10.1038/oby.2001.50
12 Chavey, C., Boucher, J., Monthouel-Kartmann, M.N., Sage, E.H., Castan-Laurell, I., Valet, P. et al. (2006) Regulation of secreted protein acidic and rich in cysteine during adipose conversion and adipose tissue hyperplasia. *Obesity* **14**, 1890–1897, https://doi.org/10.1038/oby.2006.220
13 Nie, J. and Sage, E.H. (2009) SPARC inhibits adipogenesis by its enhancement of beta-catenin signaling. *J. Biol. Chem.* **284**, 1279–1290, https://doi.org/10.1074/jbc.M808285200
14 Nie, J., Bradshaw, A.D., Delany, A.M. and Sage, E.H. (2011) Inactivation of SPARC enhances high-fat diet-induced obesity in mice. *Connect. Tissue Res.* **52**, 99–108, https://doi.org/10.3109/03008207.2010.483747

15 Shen, Y., Zhao, Y., Yuan, L., Yi, W., Zhao, R., Yi, Q. et al. (2014) SPARC is over-expressed in adipose tissues of diet-induced obese rats and causes insulin resistance in 3T3-L1 adipocytes. *Acta Histochem.* **116**, 158–166, https://doi.org/10.1016/j.acthis.2013.06.004
16 Mazzolini, G., Atorrasagasti, C., Onorato, A., Peixoto, E., Schlattjan, M., Sowa, J.P. et al. (2018) SPARC expression is associated with hepatic injury in rodents and humans with non-alcoholic fatty liver disease. *Sci. Rep.* **8**, 725, https://doi.org/10.1038/s41598-017-18981-9
17 Ryall, C.L., Viloria, K., Lhaf, F., Walker, A.J., King, A., Jones, P. et al. (2014) Novel role for matricellular proteins in the regulation of islet beta cell survival: the effect of SPARC on survival, proliferation, and signaling. *J. Biol. Chem.* **289**, 30614–30624, https://doi.org/10.1074/jbc.M114.573980
18 Wu, D., Li, L., Yang, M., Liu, H. and Yang, G. (2011) Elevated plasma levels of SPARC in patients with newly diagnosed type 2 diabetes mellitus. *Eur. J. Endocrinol.* **165**, 597–601, https://doi.org/10.1530/EJE-11-0131
19 Harries, L.W., McCulloch, L.J., Holley, J.E., Rawling, T.J., Welters, H.J. and Kos, K. (2013) A role for SPARC in the moderation of human insulin secretion. *PLoS ONE* **8**, e68253, https://doi.org/10.1371/journal.pone.0068253
20 Barreyro, F.J., Holod, S., Finocchietto, P.V., Camino, A.M., Aquino, J.B., Avagnina, A. et al. (2015) The pan-caspase inhibitor Emricasan (IDN-6556) decreases liver injury and fibrosis in a murine model of non-alcoholic steatohepatitis. *Liver Int.* **35**, 953–966, https://doi.org/10.1111/liv.12570
21 Reeves, P.G. (1997) Components of the AIN-93 diets as improvements in the AIN-76A diet. *J. Nutr.* **127**, 838S–841S, https://doi.org/10.1093/jn/127.5.838S
22 Bradshaw, A.D., Graves, D.C., Motamed, K. and Sage, E.H. (2003) SPARC-null mice exhibit increased adiposity without significant differences in overall body weight. *Proc. Natl. Acad. Sci. U. S. A.* **100**, 6045–6050, https://doi.org/10.1073/pnas.1030790100
23 Mueckler, M. and Thorens, B. (2013) The SLC2 (GLUT) family of membrane transporters. *Mol. Aspects Med.* **34**, 121–138, https://doi.org/10.1016/j.mam.2012.07.001
24 Kos, K. and Wilding, J.P. (2010) SPARC: a key player in the pathologies associated with obesity and diabetes. *Nat. Rev. Endocrinol.* **6**, 225–235, https://doi.org/10.1038/nrendo.2010.18
25 Song, H., Guan, Y., Zhang, L., Li, K. and Dong, C. (2010) SPARC interacts with AMPK and regulates GLUT4 expression. *Biochem. Biophys. Res. Commun.* **396**, 961–966, https://doi.org/10.1016/j.bbrc.2010.05.033
26 Henquin, J.C. (2000) Triggering and amplifying pathways of regulation of insulin secretion by glucose. *Diabetes* **49**, 1751–1760, https://doi.org/10.2337/diabetes.49.11.1751
27 Hamamoto, K., Yamada, S., Hara, A., Kodera, T., Seno, M. and Kojima, I. (2011) Extracellular matrix modulates insulin production during differentiation of AR42J cells: functional role of Pax6 transcription factor. *J. Cell. Biochem.* **112**, 318–329, https://doi.org/10.1002/jcb.22930
28 Guillam, M.T., Hummler, E., Schaerer, E., Yeh, J.I., Birnbaum, M.J., Beermann, F. et al. (1997) Early diabetes and abnormal postnatal pancreatic islet development in mice lacking Glut-2. *Nat. Genet.* **17**, 327–330, https://doi.org/10.1038/ng1197-327
29 Thorens, B. (2003) A gene knockout approach in mice to identify glucose sensors controlling glucose homeostasis. *Pflugers Arch.* **445**, 482–490, https://doi.org/10.1007/s00424-002-0954-2
30 Meloni, A.R., DeYoung, M.B., Lowe, C. and Parkes, D.G. (2013) GLP-1 receptor activated insulin secretion from pancreatic beta-cells: mechanism and glucose dependence. *Diab. Obes. Metab.* **15**, 15–27, https://doi.org/10.1111/j.1463-1326.2012.01663.x
31 Aye, T., Toschi, E., Sharma, A., Sgroi, D. and Bonner-Weir, S. (2010) Identification of markers for newly formed beta-cells in the perinatal period: a time of recognized beta-cell immaturity. *J. Histochem. Cytochem.* **58**, 369–376, https://doi.org/10.1369/jhc.2009.954909
32 Perez, S.E., Cano, D.A., Dao-Pick, T., Rougier, J.P., Werb, Z. and Hebrok, M. (2005) Matrix metalloproteinases 2 and 9 are dispensable for pancreatic islet formation and function in vivo. *Diabetes* **54**, 694–701, https://doi.org/10.2337/diabetes.54.3.694
33 Tremble, P.M., Lane, T.F., Sage, E.H. and Werb, Z. (1993) SPARC, a secreted protein associated with morphogenesis and tissue remodeling, induces expression of metalloproteinases in fibroblasts through a novel extracellular matrix-dependent pathway. *J. Cell Biol.* **121**, 1433–1444, https://doi.org/10.1083/jcb.121.6.1433
34 Kaido, T., Yebra, M., Cirulli, V. and Montgomery, A.M. (2004) Regulation of human beta-cell adhesion, motility, and insulin secretion by collagen IV and its receptor alpha1beta1. *J. Biol. Chem.* **279**, 53762–53769, https://doi.org/10.1074/jbc.M411202200
35 Krishnamurthy, M., Li, J., Al-Masri, M. and Wang, R. (2008) Expression and function of alphabeta1 integrins in pancretic beta (INS-1) cells. *J. Cell Commun. Signal.* **2**, 67–79, https://doi.org/10.1007/s12079-008-0030-6
36 Riopel, M., Krishnamurthy, M., Li, J., Liu, S., Leask, A. and Wang, R. (2011) Conditional beta1-integrin-deficient mice display impaired pancreatic beta cell function. *J. Pathol.* **224**, 45–55, https://doi.org/10.1002/path.2849
37 Said, N., Najwer, I. and Motamed, K. (2007) Secreted protein acidic and rich in cysteine (SPARC) inhibits integrin-mediated adhesion and growth factor-dependent survival signaling in ovarian cancer. *Am. J. Pathol.* **170**, 1054–1063